Journal of Fractional Calculus and Applications
Vol. 10(1) Jan. 2019, pp. 10-23.
ISSN: 2090-5858.
http://fcag-egypt.com/Journals/JFCA/

FRACTIONAL ORDER CLIMATE CHANGE MODEL IN A PACIFIC OCEAN

S.C. EZE, M. O. OYESANYA

Abstract. In this work, the fractional order climate change model in a Pacific Ocean is given. The model distinguishes between when damped constant $a = 0$ and when $a \neq 0$ ($a > 0$ and $a < 0$), and the solution of each case was obtained using Lindstendt-Poincare perturbation technique. The analyses of the solutions were done using MATLAB R2007b. In integer case, we observed that for damped constant $a = 0$, the oscillations become regular and tend to infinity. For $a < 0$, the amplitude increases and creates deep thermocline, which will overflow the sea and could lead to flooding. For $a > 0$, the oscillations gradually decay in amplitude toward zero. In fractional order case, we observed a clear increase and decrease in the depth of thermocline when $a < 0$ and when $a > 0$ respectively, showing a better result for studying climate change in a Pacific Ocean.

1. Introduction

Fractional order differential equations, as generalizations of classical integer order differential equations are increasingly used to model problems in applied mathematics and engineering due to their vast applications [1]. There are several investigations on fractional order differential equations, such as investigation by Gomeze et al [2], who proposed alternative procedure for constructing fractional differential equations for physical systems and used it to analyze the systems mass-spring and spring-damper in terms of fractional derivatives of Caputo type, investigations by Gomez and Balealu[3], who considered the fractional differential equation for transmission line without losses in terms of the fractional time derivatives of the Caputo type and investigation by Sergo, et a l[4], who applied the Riemann-Liouville approach and the fractional Euler-Lagrange equations in order to obtain the fractional nonlinear modeling and the numerical simulations of the oscillations of the oscillatory systems.
Recent developments in science have demonstrated that many phenomena in nature are modeled accurately using fractional derivatives[5], but fractional order differential equations for most applications hardly have exact analytic solutions, even if

2010 *Mathematics Subject Classification.* 26A33.
Key words and phrases. fractional model, Lindsted-Poincare perturbation technique, climate change, global warming, Pacific Ocean, thermocline.
Submitted Feb. 28, 2018. Revised March 8, 2018.

the exact solution of the equations can be found explicitly, it may be useless for mathematical and physical interpretation or numerical evaluation; numerical solution of the equations is one option. However, if there are large or small parameters present, the use of perturbation techniques can allow for significant progress to be made in trying to understand the solution properties. It may be possible to obtain solutions in analytical form, or reduce the equations to a much simpler set which can be tackled more easily [6].

There are numerous researches works on climate change; they function to predict the future changes in climate conditions, for examples, Fei-Fei [7] constructed a new conceptual model for ENSO based on the positive feedback of tropical ocean atmosphere interaction, White and Liu[8] analyzed the effect of EL Nino-Southern Oscillation (ENSO) on climate change and Rajapaksha et al[9] discussed how the sea surface information can be used to predict the subsurface temperature profile of the ocean. Climate change represents one of the greatest environmental threats facing planet Earth today and it has become one of the most pressing scientific challenges facing society ([10], [11]). The consequences of climate change could be devastating with increased human activities such as burning of fossil fuels, which has been identified as significant causes of recent climate change, often referred to as global warming([12], [13]). This global warming has resulted in large-scale, high-impact, nonlinear, and potentially abrupt and / or irreversible changes in physical and biological systems in the Pacific Ocean ([14], [15]).

In Pacific Ocean, the surface of the ocean absorbs most of the Suns heat in a shallow layer. This heat absorbed from the Sun increases the temperature of the surface relative to that of the deep ocean. Due to the density difference between warm and cold water, the cold water sinks down while the warm water rises. So, between the warm water and the cold water, a strong separation boundary exists, the thermocline, in between ([16], [17] and [18]). Thermocline can be shallow or deep. A shallow thermocline indicates a small amount of warm water, and a deep thermocline means there is a lot of warm water.

Because warm water takes up more space than cold water, average sea level is higher where the thermocline is deep and lower where the thermocline is shallow. The existence of deep thermocline, which its major causes is global warming has implication for the climate since it increases the average sea level rise, which poses a major threat to island nations and coastal areas, meaning that these areas could be swamped and submerged by water anytime.

Unlike the authors mentioned above, in which their analysis on climate change were on integer order derivatives, here we first analyze the integer order derivative and later move to the analysis of fractional order derivative, since fractional calculus is an important tool for the study of dynamical systems where classical methods reveal strong limitations. In this study, we shall use the proposed alternative for fractional derivative in [2] to develop the fractional order climate change model, use perturbation technique for the analytical solution and analyze the results of numerical simulations for both integer order and fractional order, and compare the results.

2. Formulation of the Climate Change Model

To formulate climate change model in a Pacific Ocean, we use the conceptual model of the tropical pacific oscillations for positive upper ocean temperature anomalies T, driving shallow thermocline depth anomalies u, which is described by the following equations ([11], [19] and [20]):

$$\frac{du}{dt} = -T + \lambda \tag{1}$$

and

$$\frac{du}{dt} = -aT + (u + bu^3) + Kcos\theta \tag{2}$$

where the constant λ is ambient noise, $Kcos\theta$ is the solar forcing, a and b are the coefficients of damping and nonlinearity respectively. By differentiating (1) with respect t and substituting in(2) , we have

$$\frac{d^2u}{dt^2} = aT - (u + bu^3) - Kcos\theta \tag{3}$$

Now substituting (1) in(3) , we have

$$\frac{d^2u}{dt^2} = a(\lambda - \frac{du}{dt}) - (u + bu^3) - Kcos\theta \tag{4}$$

.

Here, we assumed that the ambient noise is so small and negligible, and since we have solar forcing, which is soft excitation, then we expressed $K = \epsilon k$ where $k = O(1)$. We also expressed excitation$Kcos\theta = \epsilon kcos\omega(\delta t)$ in order to determine a valid asymptotic expansion. So by substituting the expression for soft excitation in (4), we have the climate model as

$$\frac{d^2u}{dt^2} = a\frac{du}{dt} + u + bu^3 + \epsilon kcos\omega(\delta t) \tag{5}$$

The motion of the system will be established by an initial disturbance (i.e., initial conditions):

$$u(0) = \frac{d}{dt}u(0) = 0 \tag{6}$$

where k is amplitude, $0 \ <\epsilon << 0 \ <1$, $0 \ <\delta << 1$ and the natural frequency ω of the system is a slowly varying function of t with right hand derivatives of all orders at $t = 0$ and is such that $\omega(0) = 0$, $|\omega|<<1$ and

$$\omega(\delta t) = 1 - e^{(-c^2\delta t)} \tag{7}$$

where $0 \ < c<<1$

3. Solution of the Model

Now to obtain the solution of (5), we shall distinguish between when damped constant $a = 0$ and when $a \neq 0$ ($a \ > 0$ and $a \ < 0$).These cases will lead us to three different types of output.

Case1 ($a = 0$): For damped constant $a = 0$, the equation (5) becomes

$$\frac{d^2u}{dt^2} = u + bu^3 + \epsilon kcos\omega(\delta t) \tag{8}$$

which is a second order, nonlinear, and non-homogeneous differential equation, with slowly varying time-dependent and periodic coefficient.

Here we use Lindstedt-Poincare idea to generalize the original time scale t as $\hat{t} = \bar{t} + 1/\delta[\mu_2(\tau)\epsilon^2 + \mu_3(\tau)\epsilon^3 + ...]$ and consider a two-time variable expansion, where the variables are:

$$\tau = \delta t, \hat{t} = \bar{t} + 1/\delta[\mu_2(\tau)\epsilon^2 + \mu_3(\tau)\epsilon^3 + ...], \bar{t} = t \tag{9}$$

From (9), we obtained the following derivatives:

$$\frac{d\tau}{dt} = \delta, \frac{\partial\hat{t}}{\partial\bar{t}} = 1, \frac{\partial\hat{t}}{\partial\tau} = 1/\delta[\mu_2\prime(\tau)\epsilon^2 + \mu_3\prime(\tau)\epsilon^3 + ...], \frac{d\bar{t}}{dt} = 1 \tag{10}$$

We now let

$$u(t;\epsilon\delta) = U(\hat{t},\tau;\epsilon\delta) \tag{11}$$

From(11) , we have

$$\frac{du}{dt} = \frac{\partial U}{\partial\hat{t}}\frac{\partial\hat{t}}{\partial\bar{t}}\frac{d\bar{t}}{dt} + \frac{\partial U}{\partial\hat{t}}\frac{\partial\hat{t}}{\partial\tau}\frac{d\tau}{dt} + \frac{\partial U}{\partial\tau}\frac{d\tau}{dt} \tag{12}$$

Now substituting(10) in (12), we have

$$\frac{du}{dt} = \frac{\partial U}{\partial\hat{t}} + \frac{\partial U}{\partial\hat{t}}[\mu_2\prime(\tau)\epsilon^2 + \mu_3\prime(\tau)\epsilon^3 + ...] + \delta\frac{\partial U}{\partial\tau} \tag{13}$$

But

$$\frac{d^2u}{dt^2} = \frac{d}{dt}(\frac{du}{dt}) \tag{14}$$

therefore

$$\frac{d^2u}{dt^2} = \frac{\partial}{\partial\hat{t}}[\frac{\partial U}{\partial\hat{t}} + \frac{\partial U}{\partial\hat{t}}[\mu_2\prime(\tau)\epsilon^2 + \mu_3\prime(\tau)\epsilon^3 + ...] + \delta\frac{\partial U}{\partial\tau}] + [\mu_2\prime(\tau)\epsilon^2 + \mu_3\prime(\tau)\epsilon^3 + ...]\frac{\partial}{\partial\hat{t}}[\frac{\partial U}{\partial\hat{t}} + \frac{\partial U}{\partial\hat{t}}[\mu_2\prime(\tau)\epsilon^2 + \mu_3\prime(\tau)\epsilon^3 + ...] + \delta\frac{\partial}{\partial\tau}[\frac{\partial U}{\partial\hat{t}} + \frac{\partial U}{\partial\hat{t}}[\mu_2\prime(\tau)\epsilon^2 + \mu_3\prime(\tau)\epsilon^3 + ...] + \frac{\partial U}{\partial\hat{t}}] \tag{15}$$

Substituting equation (15) in (8), we have

$$\begin{aligned}\frac{\partial^2 U}{\partial t^2} + 2[\mu_2\prime(\tau)\epsilon^2 + \mu_3\prime(\tau)\epsilon^3 + ...]\frac{\partial^2 U}{\partial t^2} + \delta[\mu_2\prime(\tau)\epsilon^2 + \mu_3\prime(\tau)\epsilon^3 + ...]^2\frac{\partial^2 U}{\partial t^2} + \\ 2\delta\frac{\partial^2 U}{\partial\tau^2\partial t^2} + 2\delta[\mu_2\prime(\tau)\epsilon^2 + \mu_3\prime(\tau)\epsilon^3 + ...]\frac{\partial^2 U}{\partial\tau^2\partial t^2} \\ +\delta^2\frac{\partial^2 U}{\partial\tau^2} + u + bu^3 = -\epsilon k cos\omega(\delta t)\end{aligned} \tag{16}$$

We now assume the following asymptotic series

$$U(\hat{t},\tau;\epsilon\delta) = \sum_{j=0}^{\infty}\sum_{j=0}^{\infty}U^{ij}(\hat{t},\tau)\epsilon^i\delta^j = \epsilon(U^{10}+\delta U^{11}+...)+\epsilon^2(U^{20}+\delta U^{21}+...)+... \tag{17}$$

Equating equations of order$(\epsilon^i\delta^j)$ in (16), using (17), we obtain the following equations:

$$O(\epsilon) : \frac{\partial^2 U^{10}}{\partial\hat{t}^2} + U^{10} = -\epsilon k cos\omega(\delta t) \tag{18}$$

$$O(\epsilon\delta) : \frac{\partial^2 U^{11}}{\partial\hat{t}^2} + U^{11} = -2\frac{\partial^2 U^{10}}{\partial\hat{t}\partial\tau} \tag{19}$$

$$O(\epsilon\delta^2) : \frac{\partial^2 U^{12}}{\partial\hat{t}^2} + U^{12} = -2\frac{\partial^2 U^{11}}{\partial\hat{t}\partial\tau} - \frac{\partial^2 U^{10}}{\partial\tau^2} \tag{20}$$

$$O(\epsilon^2) : \frac{\partial^2 U^{20}}{\partial\hat{t}^2} + U^{20} = 0 \tag{21}$$

$$O(\epsilon^2\delta):\frac{\partial^2 U^{21}}{\partial\hat{t}^2}+U^{21}=-2\frac{\partial^2 U^{20}}{\partial\hat{t}\partial\tau} \tag{22}$$

$$O(\epsilon^2\delta^2):\frac{\partial^2 U^{22}}{\partial\hat{t}^2}+U^{22}=-2\frac{\partial^2 U^{21}}{\partial\hat{t}\partial\tau}-\frac{\partial^2 U^{20}}{\partial\tau^2} \tag{23}$$

$$O(\epsilon^3):\frac{\partial^2 U^{30}}{\partial\hat{t}^2}+U^{30}=-b(U^{10})^3-2\mu_2\prime(\tau)\frac{\partial^2 U^{10}}{\partial\hat{t}^2} \tag{24}$$

$$O(\epsilon^3\delta):\frac{\partial^2 U^{31}}{\partial\hat{t}^2}+U^{31}=-3b(U^{10})^2U^{11}-2\frac{\partial^2 U^{30}}{\partial\hat{t}\partial\tau}-2\mu_2\prime(\tau)\frac{\partial^2 U^{11}}{\partial\hat{t}^2} \tag{25}$$

$$\begin{aligned}O(\epsilon^3\delta^2):\frac{\partial^2 U^{32}}{\partial\hat{t}^2}+U^{32}=-3b[U^{10}(U^{11})^2+(U^{10})^2U^{21}]-2\frac{\partial^2 U^{31}}{\partial\hat{t}\partial\tau}-\\ 2\mu_2\prime(\tau)\frac{\partial^2 U^{12}}{\partial\hat{t}^2}-2\mu_2\prime(\tau)\frac{\partial^2 U^{11}}{\partial\hat{t}\partial\tau}-\frac{\partial^2 U^{30}}{\partial\tau^2}\end{aligned} \tag{26}$$

etc.
Now using the scale (10) and the series (17) on initial conditions(6) , we obtain the following initial conditions in order of $(\epsilon^i\delta^j)$:

$$U^{ij}(0,0)=0\forall ij \tag{27}$$

$$O(\epsilon):\frac{\partial U^{10}(0,0)}{\partial\hat{t}}=0 \tag{28}$$

$$O(\epsilon\delta):\frac{\partial U^{11}(0,0)}{\partial\hat{t}}=-\frac{\partial U^{10}(0,0)}{\partial\tau} \tag{29}$$

$$O(\epsilon\delta^2):\frac{\partial U^{12}(0,0)}{\partial\hat{t}}=-\frac{\partial U^{11}(0,0)}{\partial\tau} \tag{30}$$

$$O(\epsilon^2):\frac{\partial U^{20}(0,0)}{\partial\hat{t}}=-\frac{\partial U^{20}(0,0)}{\partial\tau} \tag{31}$$

$$O(\epsilon^2\delta):\frac{\partial U^{21}(0,0)}{\partial\hat{t}}=-\frac{\partial U^{21}(0,0)}{\partial\tau} \tag{32}$$

$$O(\epsilon^2\delta^2):\frac{\partial U^{22}(0,0)}{\partial\hat{t}}=-\frac{\partial U^{22}(0,0)}{\partial\tau} \tag{33}$$

$$O(\epsilon^3):\frac{\partial U^{30}(0,0)}{\partial\hat{t}}+\mu_2\prime(0)\frac{\partial U^{10}(0,0)}{\partial\hat{t}}=0 \tag{34}$$

$$O(\epsilon^3\delta):\frac{\partial U^{31}(0,0)}{\partial\hat{t}}+\mu_2\prime(0)\frac{\partial U^{11}(0,0)}{\partial\hat{t}}+\frac{\partial U^{30}(0,0)}{\partial\tau}=0 \tag{35}$$

$$O(\epsilon^3\delta^2):\frac{\partial U^{32}(0,0)}{\partial\hat{t}}+\mu_2\prime(0)\frac{\partial U^{12}(0,0)}{\partial\hat{t}}+\frac{\partial U^{31}(0,0)}{\partial\tau}=0 \tag{36}$$

etc.

Therefore, using initial conditions ((27)-(38)) to solve successively the sequence of equations ((18)-(26)) , we have the approximate solution of (8) as

$$\begin{aligned} u(t;\epsilon\delta) = \epsilon[a_{10}(0)cos\hat{t} + A(\tau) + \delta[b_{11}(0)sin\hat{t}] + \delta^2[a_{12}(0)cos\hat{t}- \\ A''(\tau) + ... + \epsilon^3[a_{30}(0)cos\hat{t} + b[r_1(\tau) + r_2(\tau)cos2\hat{t} + r_3(\tau)cos3\hat{t}]+ \\ \delta[a_{31}(0)cos\hat{t} + b_{31}(0)sin\hat{t} - \frac{1}{3}r_4(\tau)sin2\hat{t} - \frac{1}{8}r_5(\tau)sin3\hat{t}]+ \\ \delta^2[a_{32}(0)cos\hat{t} + b_{32}(0)sin\hat{t} + r_6(\tau) - \frac{1}{3}r_7cos2\hat{t}- \\ \frac{1}{3}r_8(\tau)sin2\hat{t} - \frac{1}{8}r_{10}(\tau)sin3\hat{t}] + ...]] + O(\epsilon^4) \end{aligned} \tag{37}$$

where all the parameters in(37) are defined in (38) bellow

$$\begin{aligned} A(\tau) &= -kcos\omega(\tau), \\ a_{10}(0) &= -A(0), \\ b_{11}(0) &= -A'(0), \\ a_{12}(0) &= -A''(0), \\ a_{30}(0) &= \frac{95A(0)^3}{32}b, \\ b_{31}(0) &= \frac{2}{3}r_4(0) + \frac{3}{8}r_5(0), \\ a_32(0) &= -r_6(0), \\ b_{32}(0) &= \frac{1}{6}r_8(0) + \frac{1}{24}r_{10}(0) + \mu_2\prime(0), \\ r_1(\tau) &= -(A^3 + \frac{3a_{10}^2A}{2}), \\ r_2(\tau) &= -\frac{3a_{10}^2A}{2}, \\ r_3(\tau) &= -\frac{3a_{10}^3}{32}, \\ r_4(\tau) &= -3bb_{11}^2Aa_{10} + 4r_2\prime b, \\ r_5(\tau) &= \frac{-3}{4}bb_{11}^2a_{10}^2 + 6r_2\prime b, \\ r_6(\tau) &= \frac{1}{2}Ab_{11} + 2a_{10}AA'' + \frac{1}{2}a_{10}^2A'' - A^2A'' - br_1\prime\prime(\tau), \\ r_7(\tau) &= a_{10}AA'' - \frac{1}{2}Ab_{11} - \frac{1}{2}a_{10}^2A'' - br_2\prime\prime(\tau), \\ r_8(\tau) &= \frac{4}{3}r_4'(\tau)b, \\ r_9(\tau) &= \frac{1}{4}a_{10}^2A'' - \frac{1}{4}a_{10}b_{11} - br_1''(\tau), \\ r_{10}(\tau) &= \frac{3}{4}br_5'(\tau). \end{aligned} \tag{38}$$

Case 2. $a \neq 0$ ($a \ > 0$ and $a \ < 0$): For damped constant $a \neq 0$, the equation (5) becomes

$$\frac{d^2u}{dt^2} + a\frac{du}{dt} + u + bu^3 = -\epsilon kcos\omega(\delta t), a \neq 0 \tag{39}$$

which is forced cubic Duffing equation.
Now substituting (11) , (13) and (15) in equation (39), we have

$$\begin{aligned}&\frac{\partial^2 U}{\partial \hat{t}^2}+2\phi(\epsilon)\frac{\partial^2 U}{\partial \hat{t}^2}+\delta\phi^2(\epsilon)\frac{\partial^2 U}{\partial \hat{t}^2}+2\delta\frac{\partial^2 U}{\partial \tau\partial t}+2\delta\phi(\epsilon)\frac{\partial^2 U}{\partial \tau\partial t}+\\ &\delta^2\frac{\partial^2 U}{\partial \tau^2}+\alpha[\frac{\partial U}{\partial \hat{t}}+\frac{\partial U}{\partial \hat{t}}\phi(\epsilon)+\delta\frac{\partial U}{\partial \tau}]+U+bU^3=-\epsilon k cos\omega(\delta t)\end{aligned} \tag{40}$$

where $\phi(\epsilon)=\mu_2\prime(\tau)\epsilon^2+\mu_3\prime(\tau)\epsilon^3+...$
Equating equations of order$(\epsilon^i\delta^j)$ in(40), using (17), we obtain the following equations:

$$O(\epsilon):\frac{\partial^2 U^{10}}{\partial \hat{t}^2}+a\frac{\partial U^{10}}{\partial \hat{t}}+U^{10}=-\epsilon k cos\omega(\delta t) \tag{41}$$

$$O(\epsilon\delta):\frac{\partial^2 U^{11}}{\partial \hat{t}^2}+a\frac{\partial U^{11}}{\partial \hat{t}}+U^{11}=-2\frac{\partial^2 U^{10}}{\partial \hat{t}\partial \tau}+a\frac{\partial U^{10}}{\partial \tau} \tag{42}$$

$$O(\epsilon\delta^2):\frac{\partial^2 U^{12}}{\partial \hat{t}^2}+a\frac{\partial U^{12}}{\partial \hat{t}}+U^{12}=-2\frac{\partial^2 U^{11}}{\partial \hat{t}\partial \tau}-\frac{\partial^2 U^{10}}{\partial \tau^2}-a\frac{\partial U^{11}}{\partial \tau} \tag{43}$$

$$O(\epsilon^2):\frac{\partial^2 U^{20}}{\partial \hat{t}^2}+a\frac{\partial U^{20}}{\partial \hat{t}}+U^{20}=0 \tag{44}$$

$$O(\epsilon^2\delta):\frac{\partial^2 U^{21}}{\partial \hat{t}^2}+a\frac{\partial U^{21}}{\partial \hat{t}}+U^{21}=-2\frac{\partial^2 U^{20}}{\partial \hat{t}\partial \tau}-a\frac{\partial U^{20}}{\partial \tau} \tag{45}$$

$$O(\epsilon^2\delta^2):\frac{\partial^2 U^{22}}{\partial \hat{t}^2}+a\frac{\partial U^{22}}{\partial \hat{t}}+U^{22}=-2\frac{\partial^2 U^{21}}{\partial \hat{t}\partial \tau}-\frac{\partial^2 U^{20}}{\partial \tau^2}-a\frac{\partial U^{21}}{\partial \tau} \tag{46}$$

$$O(\epsilon^3):\frac{\partial^2 U^{30}}{\partial \hat{t}^2}+a\frac{\partial U^{30}}{\partial \hat{t}}+U^{30}=-b(U^{10})^3-2\mu_2\prime(\tau)\frac{\partial^2 U^{10}}{\partial \hat{t}^2}-a\mu_2\prime(\tau)\frac{\partial^2 U^{10}}{\partial \tau\partial \hat{t}} \tag{47}$$

$$\begin{aligned}&O(\epsilon^3\delta):\frac{\partial^2 U^{31}}{\partial \hat{t}^2}+a\frac{\partial U^{31}}{\partial \hat{t}}+U^{31}=-3b(U^{10})^2U^{11}-\\ &2\frac{\partial^2 U^{30}}{\partial \hat{t}\partial \tau}-2\mu_2\prime(\tau)\frac{\partial^2 U^{11}}{\partial \hat{t}^2}-a\mu_2\prime(\tau)\frac{\partial^2 U^{11}}{\partial \tau\partial \hat{t}}-a\frac{\partial U^{30}}{\partial \tau}\end{aligned} \tag{48}$$

$$\begin{aligned}O(\epsilon^3\delta^2):&\frac{\partial^2 U^{32}}{\partial \hat{t}^2}+a\frac{\partial U^{32}}{\partial \hat{t}}+U^{32}=-3b[U^{10}(U^{11})^2+(U^{10})^2U^{21}]-2\frac{\partial^2 U^{31}}{\partial \hat{t}\partial \tau}-\\ &2\mu_2\prime(\tau)\frac{\partial^2 U^{12}}{\partial \hat{t}^2}-2\mu_2\prime(\tau)\frac{\partial^2 U^{11}}{\partial \hat{t}\partial \tau}-\frac{\partial^2 U^{30}}{\partial \tau^2}-a\mu_2\prime(\tau)\frac{\partial^2 U^{12}}{\partial \tau\partial \hat{t}}-a\frac{\partial U^{31}}{\partial \tau}\end{aligned} \tag{49}$$

etc
Therefore, using initial conditions ((27)-(36)) to solve successively the sequence of

equations ((42)-((49)), we have the approximate solution of (39) as

$$\begin{aligned}
u(t;\epsilon\delta) = {} & \epsilon[a_0 e^{c_1\hat{t}} + b_0(0)e^{c_2\hat{t}} + A(\tau) + \delta[a_1(0)e^{c_1\hat{t}} + b_1(0)e^{c_2\hat{t}} - aA'(\tau)] \\
& +\delta^2[a_2 e^{c_1\hat{t}} + b_2(0)e^{c_2\hat{t}} - (a-1)A''(\tau)] + ...] + \epsilon^3[a_6(0)e^{c_1\hat{t}} + b_6(0)e^{c_2\hat{t}}] \\
& +b[h_1(\tau)e^{3c_1\hat{t}} + h_2(\tau)e^{(2c_1+c_2)\hat{t}} + h_3(\tau))e^{(c_1+2c_2)\hat{t}} + h_4(\tau)e^{3c_2\hat{t}} \\
& +h_5(\tau)e^{2c_1\hat{t}} + h_6(\tau)e^{(c_1+c_2)\hat{t}} + h_7(\tau)e^{2c_2\hat{t}} + h_8(\tau)] + \delta[a_7(0)e^{c_1\hat{t}} \\
& +b_7(0)e^{c_2\hat{t}} + b[h_9(\tau)e^{3c_1\hat{t}} + h_{10}(\tau)e^{3c_2\hat{t}} + h_{11}(\tau)e^{(2c_1+c_2)\hat{t}} \\
& +h_{12}(\tau)e^{(c_1+2c_2)\hat{t}} + h_{13}(\tau))e^{2c_1\hat{t}} + h_{14}(\tau)e^{(c_1+c_2)\hat{t}} \\
& +h_{15}(\tau)e^{2c_2)\hat{t}} + h_{16}(\tau)]] + \delta^2[a_8(0)e^{c_1\hat{t}} \\
& +b_8(0)e^{c_2\hat{t}} + b[[h_{17}(\tau)e^{3c_1\hat{t}} + h_{18}(\tau)e^{3c_2\hat{t}} \\
& +h_{19}(\tau)e^{(2c_1+c_2)\hat{t}} + h_{20}(\tau)e^{(c_1+2c_2)\hat{t}} \\
& +h_{21}(\tau))e^{2c_1\hat{t}}h_{22}(\tau)e^{(c_1+c_2)\hat{t}} \\
& +h_{23}(\tau)e^{2c_2)\hat{t}} + h_{24}(\tau)] + ...]] \\
& +O(\epsilon^4)
\end{aligned} \tag{50}$$

where all the parameters in(50) are defined bellow:
$a_0(0) = \frac{-A(0)c_2}{c_2-c_1}, b_0(0) = \frac{A(0)c_2}{c_2-c_1}, a_1(0) = \frac{aA'(0)c_2}{c_2-c_1}, b_1(0) = \frac{aA'(0)c_1}{c_2-c_1}$,
$a_2(0) = \frac{-(a+1)A''(0)c_2}{c_2-c_1}$,
$b_2(0) = \frac{(a+1)A''(0)c_1}{c_2-c_1}, a_6(0) = \frac{-bc_2H_1(0)+bH_2(0)}{c_2-c_1}, b_6(0) = \frac{-bH_2(0)+bc_1H_1(0)}{c_2-c_1}$,
$a_7(0) = \frac{-bc_2H_3(0)+bH_4(0)}{c_2-c_1}, b_7(0) = \frac{-bH_4(0)+bc_1H_3(0)}{c_2-c_1}, a_8(0) = \frac{-bc_2H_5(0)+bH_6(0)}{c_2-c_1}, b_8(0) = \frac{-bH_6(0)+bc_1H_5(0)}{c_2-c_1}, c_1 = \frac{-a+\sqrt{a^2-4}}{2}, c_2 = \frac{-a-\sqrt{a^2-4}}{2}, A(0) = -k, h_1(\tau) = -a_0^3, h_2(\tau) = -3a_0^2b_0, h_3(\tau) = -3a_0^2b_0^2, h_4(\tau) = -b_0^3, h_5(\tau) = -3Aa_0^2, h_6(\tau) = -6Aa_0b_0, h_7(\tau) = -3Ab_0^2, h_8(\tau) = -A^3, h_9(\tau) = -(3a_0^2a_1 + 6c_1h_1' - ah_1'), h_{10}(\tau) = -(3b_0^2b_1 + 6c_2h_4' - ah_4'), h_{11}(\tau) = -(6a_0a_1b_0 + 3a_0^2b_1 + 4c_1h_2' + 2c_2h_2' - ah_2'), h_{12}(\tau) = -(3a_1b_0^2 + 6a_0b_0b_1 - 2c_1h_3' - 4c_2h_3' - ah_3'), h_{13}(\tau) = -(6Aa_0a_1 - 3aA'a_0^2 - 4c_1h_5' - ah_5'), h_{14}(\tau) = -(6Aa_1b_0 + 6Aa_0b_1 - 6aAa_0b_0 - 2c_1h_6' - 2c_2h_6' - ah_6'), h_{15}(\tau) = -(6Ab_0b_1 - 3aA'a_0b_0^2 - 4c_2h_7' - ah_7'), h_{16}(\tau) = -(3aA^2A' - 2h_8' + ah_8'), h_{17}(\tau) = -(3a_0a_1^2 + 6a_0^2a_2 + 6c_1h_9' + h_1'' + ah_9'), h_{18}(\tau) = -(3b_0b_1^2 + 3b_0^2b_2 + 6c_2h_{10}' + h_4'' + ah_{10}'), h_{19}(\tau) = -[3a_0b_1^2 + 3a_1^2b_0 + 6a_1b_0b_1 + 3a_2b_0^2 + 6a_0b_0b_2 + 2(2c_1+c_2)h_{11}' + h_2'' + ah_{11}'], h_{20}(\tau) = -[3a_0b_1^2 + 3a_1^2b_0 + 6a_1b_0b_1 + 3a_2b_0^2 + 6a_0b_0b_2 + 2(2c_1+c_2)h_{12}' + h_3'' + ah_{12}'], h_{21}(\tau) = -[-6aA'a_0a_1 + 3Aa_1^2 + 6Aa_0a_2 - 3a(a+1)A''a_0^2 + 4c_1h_{13}' + h_5'' + ah_{13}'], h_{22}(\tau) = -[-6aA'a_0b_1 - 6aA'a_1b_0 + 6Aa_1b_1 + 6Aa_2b_0 + 6Aa_0b_2 - 6a(a+1)A''a_0b_0 + 2(c_1+c_2)h_{14}' + h_6'' + ah_{14}'], h_{23}(\tau) = -[-6aA'b_0b_1 + 3Ab_1^2 + 6Ab_0b_2 - 3a(a+1)A''b_0^2 + 4c_2h_{15}' + h_7'' + ah_{15}'], h_{24}(\tau) = 3a^2AA^{2\prime} - 3a(a+1)A^2A'' + h_8'' + ah_{16}'], H_1(0) = h_1(0) + h_2(0) + h_3(0) + h_4(0) + h_5(0) + h_6(0) + h_7(0) + h_8(0), H_2(0) = h_1(0)3c_1 + h_2(0)(2c_1+c_2) + h_3(0)(c_1+2c_2) + h_4(0)3c_2 + h_5(0)2c_1 + h_6(0)(c_1+c_2) + h_7(0)2c_2, H_3(0) = h_9(0) + h_{10}(0) + h_{11}(0) + h_{12}(0) + h_{13}(0) + h_{14}(0) + h_{15}(0) + h_{16}(0), H_4(0) = h_9(0)3c_1 + h_{10}(0)3c_2 + h_{11}(0)(2c_1 + c_2) + h_{12}(0)(c_1+2c_2) + h_{13}(0)2c_1 + h_{14}(0)(c_1+c_2) + h_{15}(0)2c_2, H_5(0) = h_{17}(0) + h_{18}(0) + h_{19}(0) + h_{20}(0) + h_{21}(0) + h_{22}(0) + h_{23}(0) + h_{24}(0)$ and $H_6(0) = h_{17}(0)3c_1 + h_{18}(0)3c_2 + h_{19}(0)(2c_1+c_2) + h_{20}(0)(c_1+2c_2) + h_{21}(0)2c_1 + h_{22}(0)(c_1+c_2) + h_{23}(0)2c_2$.

4. Fractional Formulation of the Climate Change Model

We shall use the proposed fractional operator in [2] to describe the climate change model.The idea is to introduce an additional parameter σ, which must have dimension of seconds and consistent with the dimension of the ordinary derivative operators.
Now using the proposed idea, we have

$$\begin{aligned} \frac{d}{dt} &\rightarrow \frac{1}{\sigma^{1-\beta}}\frac{d^{\beta}}{dt^{\beta}},\ 0\ <\beta\ \leq 1 \\ \frac{d^2}{dt^2} &\rightarrow \frac{1}{\sigma^{2-\alpha}}\frac{d^{\alpha}}{dt^{\alpha}},\ 1\ <\beta\ \leq 2 \end{aligned} \tag{51}$$

Using (51) , the climate model (5) can be written in terms of fractional time derivatives as:

$$\frac{1}{\sigma^{2-\alpha}}\frac{d^{\alpha}u}{dt^{\alpha}} + a\frac{1}{\sigma^{1-\beta}}\frac{d^{\beta}u}{dt^{\beta}} + u + bu^3 = -\epsilon k cos\omega(\delta t) \tag{52}$$

$\implies \frac{d^{\alpha}u}{dt^{\alpha}} + a\sigma^{1+\beta-\alpha}\frac{d^{\beta}u}{dt^{\beta}} + \sigma^{2-\alpha}u + b\sigma^{2-\alpha}u^3 = -\epsilon k\sigma^{2-\alpha}cos\omega(\delta t)$
We now let $\sigma^{1+\beta-\alpha} = m$ seconds and $2-\alpha = n$ seconds to have
$\frac{d^{\alpha}u}{dt^{\alpha}} + am\frac{d^{\beta}u}{dt^{\beta}} + nu + bnu^3 = -\epsilon kncos\omega(\delta t)$

$$\implies D_t^{\alpha}u + amD_t^{\beta}u + nu + bnu^3 = -\epsilon kncos\omega(\delta t) \tag{53}$$

with initial conditions

$$u(0) = D^{\beta}u(0) = 0 \tag{54}$$

where the symbols D_t^{α} and D_t^{β} are describing the orders of the fractional time derivatives.

5. Solution of Fractional Formulation of the Climate Change Model

Now to obtain the solution of (53), we shall distinguish between when damped constant $a = 0$ and when $a \neq 0$ ($a\ > 0$ and $a\ < 0$). These cases will lead us to three different types of output.
Case1 ($a = 0$): For damped constan t$a = 0$, the equation (53) becomes

$$D_t^{\alpha}u + nu + bnu^3 = -\epsilon kncos\omega(\delta t) \tag{55}$$

Using (13), we have
$[D_t^{\alpha}u = \frac{\partial U}{\partial \hat{t}} + \phi(\epsilon)\frac{\partial U}{\partial \hat{t}} + \delta\frac{\partial U}{\partial \tau}]^{\alpha}$

$$\begin{aligned} \implies D_t^{\alpha}u = D_{\hat{t}}^{\alpha}U + \alpha\phi(\epsilon)D_{\hat{t}}^{\alpha}U + \alpha\delta D_{\hat{t}}^{\alpha-1}UU_{\tau} + \frac{1}{2}\alpha(\alpha-1)\phi^2(\epsilon)D_{\hat{t}}^{\alpha}U \\ +\alpha(\alpha-1)\delta\phi(\epsilon)D_{\hat{t}}^{\alpha-2}UU_{\hat{t}\tau} + \frac{1}{2}\alpha(\alpha-1)\delta^2 D_{\hat{t}}^{\alpha-2}UU_{\tau\tau} + ... \end{aligned} \tag{56}$$

were $\phi(\epsilon) = \mu_2\prime(\tau)\epsilon^2 + \mu_3\prime(\tau)\epsilon^3 + ...$
Substituting (56) in (55), we have

$$\begin{aligned} D_{\hat{t}}^{\alpha}U + \alpha\phi(\epsilon)D_{\hat{t}}^{\alpha}U + \alpha\delta D_{\hat{t}}^{\alpha-1}UU_{\tau} + \frac{1}{2}\alpha(\alpha-1)\phi^2(\epsilon)D_{\hat{t}}^{\alpha}U \\ +\alpha(\alpha-1)\delta\phi(\epsilon)D_{\hat{t}}^{\alpha-2}UU_{\hat{t}\tau} + \frac{1}{2}\alpha(\alpha-1)\delta^2 D_{\hat{t}}^{\alpha-2}UU_{\tau\tau} \\ +... + nU + nbU^3 = -\epsilon kncos\omega(\delta t) \end{aligned} \tag{57}$$

Equating equations of order($\epsilon^i\delta^j$) in (57), using the series (17), we obtain the following equations:

$$O(\epsilon): D_{\hat{t}}^{\alpha}U^{10} + nU^{10} = -kncos\omega(\tau) \tag{58}$$

$$O(\epsilon\delta): D_{\hat{t}}^{\alpha}U^{11} + nU^{11} = -\alpha D_{\hat{t}}^{\alpha-1}(U_{\tau}^{10}) \tag{59}$$

$$O(\epsilon^2): D_{\hat{t}}^{\alpha}U^{20} + nU^{20} = 0 \tag{60}$$

$$O(\epsilon^2\delta): D_{\hat{t}}^{\alpha}U^{21} + nU^{21} = -\alpha D_{\hat{t}}^{\alpha-1}(U_{\tau}^{20}) \tag{61}$$

etc

Now using the scale (10) and the series (17) on initial conditions (54), we obtain the following initial conditions in order of ($\epsilon^i\delta^j$):

$$U^i j(0,0) = 0 \forall ij \tag{62}$$

$$O(\epsilon): D_{\hat{t}}^{\beta}U^{10}(0,0) = 0 \tag{63}$$

$$O(\epsilon\delta): D_{\hat{t}}^{\beta}U^{11}(0,0) = -U_{\tau}^{10}(0,0) \tag{64}$$

$$O(\epsilon^2): D_{\hat{t}}^{\beta}U^{20}(0,0) = -U_{\tau}^{20}(0,0) \tag{65}$$

$$O(\epsilon^2\delta): D_{\hat{t}}^{\beta}U^{21}(0,0) = -U_{\tau}^{21}(0,0) \tag{66}$$

etc

Therefore, taking Laplace transform and using initial conditions (62)-(66) to solve successively the sequence of equations ((58)-(61)), we have the approximate solution of (55) as

$$\begin{aligned} u(t;\epsilon\delta) = \epsilon[-kncos\omega(\tau)\mathcal{L}^{-1}[\frac{1}{s(s^{\alpha}+n)}]+ \\ \delta\mathcal{L}^{-1}[\frac{1}{(s^{\alpha}+n)}\mathcal{L}[-\alpha D_{\hat{t}}^{\alpha-1}[kncos\omega'(\tau)\mathcal{L}^{-1}[\frac{1}{s(s^{\alpha}+n)}]]]] + O(\epsilon^2)] \end{aligned} \tag{67}$$

where $\mathcal{L}$ is a Laplace transform operator.

But using Mittag-Leffler function, that is $E_{\alpha,\beta}(z) = \sum_{i=0}^{\infty} \frac{z^i}{\Gamma(\alpha i+\beta)}$, we have

$$\mathcal{L}^{-1}[\frac{1}{s(s^{\alpha}+n)}] = t^{\alpha}E_{\alpha,\alpha+1}(-nt^{\alpha}) = \sum_{i=0}^{\infty}\frac{(-nt^{\alpha})^i}{\Gamma(\alpha i+\alpha+1)} \tag{68}$$

Case 2. $a \neq 0$ ($a > 0$ and $a < 0$): For damped constant $a \neq 0$, the equation (53) becomes

$$D_t^{\alpha}u + amD_t^{\beta}u + nu + bnu^3 = -\epsilon kncos\omega(\delta t),\ 0 < \beta \leq 1\ ,\ 1 < \beta \leq 2 \tag{69}$$

Now using (56) on (69), we have

$$\begin{aligned} D_{\hat{t}}^{\alpha}U + \alpha\phi(\epsilon)D_{\hat{t}}^{\alpha}U + \alpha\delta D_{\hat{t}}^{\alpha-1}UU_{\tau} + \frac{1}{2}\alpha(\alpha-1)\phi^2(\epsilon)D_{\hat{t}}^{\alpha}U \\ +\alpha(\alpha-1)\delta\phi(\epsilon)D_{\hat{t}}^{\alpha-2}UU_{\hat{t}\tau} + \frac{1}{2}\alpha(\alpha-1)\delta^2D_{\hat{t}}^{\alpha-2}UU_{\tau\tau} + ... \\ +am[D_{\hat{t}}^{\beta}U + \beta\phi(\epsilon)D_{\hat{t}}^{\beta}U + \beta\delta D_{\hat{t}}^{\beta-1}UU_{\tau} + \frac{1}{2}\beta(\beta-1)\phi^2(\epsilon)D_{\hat{t}}^{\beta}U \\ +\beta(\beta-1)\beta\phi(\epsilon)D_{\hat{t}}^{\beta-2}UU_{\hat{t}\tau} + \frac{1}{2}\beta(\beta-1)\beta^2D_{\hat{t}}^{\beta-2}UU_{\tau\tau} + ...] \\ +nU + bnU^3 = -\epsilon nkcos\omega(\tau) \end{aligned} \tag{70}$$

Equating equations of order($\epsilon^i\delta^j$) in (70), using the series (17), we obtain the following equations:

$$O(\epsilon) : D_{\hat{t}}^{\alpha}U^{10} + amD_{\hat{t}}^{\beta}U^{10} + nU^{10} = -kncos\omega(\tau) \tag{71}$$

$$O(\epsilon\delta) : D_{\hat{t}}^{\alpha}U^{11} + amD_{\hat{t}}^{\beta}U^{11} + nU^{11} = -\alpha D_{\hat{t}}^{\alpha-1}(U_{\tau}^{10}) + aU_{\tau}^{10} \tag{72}$$

$$O(\epsilon^2) : D_{\hat{t}}^{\alpha}U^{20} + amD_{\hat{t}}^{\beta}U^{20} + nU^{20} = 0 \tag{73}$$

$$O(\epsilon^2\delta) : D_{\hat{t}}^{\alpha}U^{21} + amD_{\hat{t}}^{\beta}U^{21} + nU^{21} = -\alpha D_{\hat{t}}^{\alpha-1}(U_{\tau}^{20}) + aU_{\tau}^{20} \tag{74}$$

etc

Therefore, taking Laplace transform and using initial conditions ((62)-(66)) to solve successively the sequence of equations ((71)-(74)), we have the approximate solution of (69) as

$$u(t;\epsilon\delta) = \epsilon[-kncos\omega(\tau)\mathcal{L}^{-1}[\frac{1}{s(s^{\alpha}+ams^{\beta}+n)}]+$$

$$\delta\mathcal{L}^{-1}[\frac{1}{(s^{\alpha}+ams^{\beta}+n)}\mathcal{L}[-\alpha D_{\hat{t}}^{\alpha-1}[kncos\omega'(\tau)\mathcal{L}^{-1}[\frac{1}{s(s^{\alpha}+ams^{\beta}+n)}+...]]]]]+O(\epsilon^2) \tag{75}$$

6. Numerical Simulations and Discussion of Results

The numerical simulations of the approximate solutions (37), (50), (67) and (75) are presented below, with various values of α, β, δ and a.

The first part of the simulations deal with the solution of the integer order derivative of the climate model. In Figure1, the graph of depth against time for values of damping constants a=-0.2,-0.5, and -0.8 were plotted, and the results showed that we have sinusoidal curves whose amplitudes are increasing as a result of under-damping. Figure 2 deals with a free oscillation, that is, without the presence of damping. When the solution (37) was simulated, the result showed that the solution displays expected behavior, that is, an oscillation whose amplitude is maintained due to the absence of damping. In this Figure 2, damping constant a=0, and the sinusoidal curves show regular oscillations for values of δ=0.02,0.05 and 0.08. The curves coincided as a result of small values of $\delta(0 < \delta \leq 1)$. But simulating using the same values of δ=0.02,0.05 and 0.08, and the values of ϵ =0.01,0.001 and 0.0001 respectively, we have figure 3, which have slight changes in the oscillations as ϵ increases.

When the solution(50) was simulated; the result shows that the solution loses the oscillatory characteristics and the amplitudes decreases very fast. In Figure 4, we observed that for values of $\epsilon = 0.1, 0.01, 0.0014$, and damping constant $a = 0.2$, the oscillations decreases in amplitude. With zero damping constant as shown in figure 2, we have the usual sinusoidal curves, but as the damping constant increases as shown in Figure 4, the oscillations gradually decay in amplitude towards zero. That means after a sufficiently long time, the output corresponding to a purely sinusoidal input will practically be a harmonic oscillation whose frequency is that of the input.

When the damping constant is so large, as in the case of Figure 5 for $a = 2$, we observed that there is no oscillations. This is physically understandable since the

damping takes energy from system and there is no external force that keeps the oscillations going. But as the values of ϵ increases (from $\epsilon = 0.001$ to $\epsilon = 0.1$) as in Figure 6, which showed the increase in the external force, then $a = 2$ oscillate and dies away quickly since the effect is very small. In Figure 7, we observed that when $a = 0$, the oscillations are regular and tend to infinity, which led to permanent thermocline. When $a < 0$, the amplitude increases and leads to increase in the depth of thermocline, which could lead to flooding. When $a > 0$, the oscillations are still sinusoidal but the amplitude decreases slowly towards equilibrium, and that helped to control the depth of the thermocline.
The effect of climate change in a Pacific Ocean may be well understood if we consider the solution of the fractional order model, as in the second part of the simulations. In this part, the effects of fractional order on the behavior of the solutions (67) and (75) were investigated.
Figure 8 shows that the trajectories for δ=0.02,0.05 and 0.08 coincided for α=3/2 , but simulating using the same values of δ=0.02,0.05 and 0.08 , and the values of ϵ=0.01,0.001 and 0.0001 respectively, as shown in Figure 9, the trajectory increases as ϵ increases, which shows the increase in the external force. From Figure 10, it can be observed that for α=5/4, 3/2 and 7/4 , the fractional order exhibits a significant effect by increasing the trajectory as α increases. Figure 11 shows that for a=0.2, α=3/2, β=1/2, and the values of δ=0.02,0.05 and 0.08, the trajectories coincided, but simulating using the same parameters and damped constant $a = -0.2$, as in Figure 12, the trajectory increases as time increases. Figure 13 shows that when the fractional order increases, the trajectory decreases for $a = 0.2$, but in Figure 14, the trajectory decreases as a result of under-damping. Figures 15 shows that with damped constant $a = 0.2$ and β fixed, the trajectory decreases as α increases. But in Figure 16, with under-damped constant $a = -0.2$ and β fixed, the trajectory increases as α increases.
Thus, in this work, the numerical simulations realized from the fractional order system seem to show a better result in studying the climate change in a Pacific Ocean. That means if the choice of the orders of α and β of the derivatives are conveniently made, a model with fractional order derivatives will give a better result in studying the climate change in a Pacific Ocean.

7. Conclusion

In this work, we have formulated the mathematical model that will advance the climate model by capturing fractional order derivatives. The fractional order derivatives in the model made the model difficult to solve exactly. So since there were small parameters present, we used perturbation technique which allowed significant progress to be made in trying to understand the solution properties. In this study, we obtained a model where a simplistic approach for extracting a solution failed as a result of non-uniformity, which manifests itself in the presence of so-called secular terms. So because of this non-uniformity, we adapted the Lindstedt-Poincare perturbation technique, which helped to prevent the appearance of secular terms. We discussed the analytical solution of the integer order model by distinguishing between damped constant $a = 0$ and$a \neq 0$ ($a > 0$ and $a < 0$), which led us to three different types of output. Our analysis was done using MATLAB software, and we observed that when $a = 0$, the oscillations are regular and tend to infinity. For $a < 0$, the amplitude increases and could lead to flooding. For $a > 0$, the

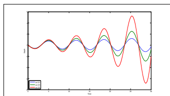

Figure 1: Graph of depth against time for values of $a = -0.2, -0.5$ and -0.8. The parameters used are $b = 1, c = 0.1, k = 6, \delta = 0.001$ and $\varepsilon = 0.01$.

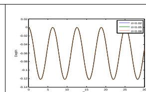

Figure 2: Graph of depth against time for values of $\delta = 0.02,\ 0.05$ and 0.08. The parameters used are $b = 1, c = 0.1, k = 6$ and $\varepsilon = 0.01$.

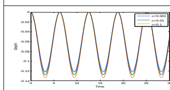

Figure 3: Graph of depth against time for values of $\delta = 0.02, 0.05, 0.08$ and $\varepsilon = 0.01, 0.001, 0.0001$. The parameters used are $b = 1, c = 0.1$ and $k = 6$.

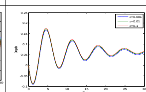

Figure 4: Graph of depth against time for values of $\varepsilon = 0.1,\ 0.01$ and 0.001. The parameters used are $a = 0.2, b = 1, c = 0.1, k = 6$ and $\delta = 0.01$.

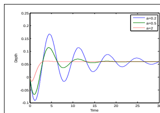

Figure 5: Graph of depth against time for values of $a = 0.2,\ 0.5$ and 2. The parameters used are $b = 1, c = 0.1, k = 6, \delta = 0.01$ and $\varepsilon = 0.001$.

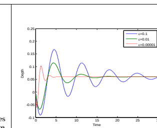

Figure 6: Graph of depth against time for values of $\varepsilon = 0.001,\ 0.01$ and 0.1. The parameters used are $a = 0.2, 0.5, 2, b = 1, c = 0.1, k = 6$ and $\delta = 0.01$.

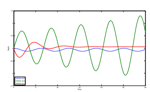

Figure 7: Graph of depth against time for values of $a = 0,\ 0.5$ and -0.2. The parameters used are $b = 1, c = 0.1, k = 6, \delta = 0.001$ and $\varepsilon = 0.01$.

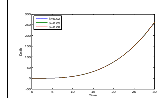

Figure 8: Graph of depth against time for values of $\delta = 0.02,\ 0.05$ and 0.08. The parameters used are $b = 1, c = 0.1, k = 6, n = 2, \varepsilon = 0.01$ and $\alpha = \frac{3}{2}$.

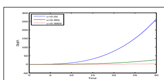

Figure 9: Graph of depth against time for values of $\delta = 0.01, 0.001,\ 0.0001,$ and $\varepsilon = 0.001, 0.01,\ 0.1$. The parameters used are $= 1, c = 0.1, k = 6, n = 2$ and $\alpha = \frac{3}{2}$.

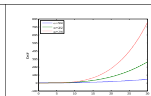

Figure 10: Graph of depth against time for values of $\alpha = {}^{5}/_{4},\ {}^{3}/_{2}$ and ${}^{7}/_{4}$. The parameters used are $b = 1, c = 0.1, k = 6, n = 2, \delta = 0.01$ and $\varepsilon = 0.001$.

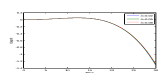

Figure 11: Graph of depth against time for values of $\delta = 0.02,\ 0.05$ and 0.08. The parameters used are $a = 0.2, b = 1, c = 0.1, k = 6, m = 1, n = 2, \varepsilon = 0.01, \alpha = \frac{3}{2}$ and $\beta = \frac{1}{2}$.

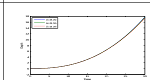

Figure 12: Graph of depth against time for values of $\delta = 0.02,\ 0.05$ and 0.08. The parameters used are $a = -0.2, b = 1, c = 0.1, k = 6, m = 1, n = 2, \varepsilon = 0.01, \alpha = \frac{3}{2}$ and $\beta = \frac{1}{2}$.

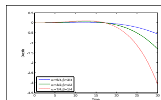

Figure 13: Graph of depth against time for values of $\alpha = {}^{5}/_{4}, \beta = {}^{3}/_{4},\ \alpha = {}^{3}/_{2}, \beta = {}^{1}/_{2}$ and $\alpha = {}^{7}/_{4}, \beta = {}^{1}/_{4}$. The parameters used are $a = 0.2, b = 1, c = 0.1, k = 6, m = 1, n = 2$ and $\delta = 0.01$.

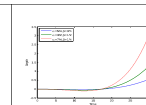

Figure 14: Graph of depth against time for values of $\alpha = {}^{5}/_{4}, \beta = {}^{3}/_{4},\ \alpha = {}^{3}/_{2}, \beta = {}^{1}/_{2}$ and $\alpha = {}^{7}/_{4}, \beta = {}^{1}/_{4}$. The parameters used are $a = -0.2, b = 1, c = 0.1, k = 6, m = 1, n = 2$ and $\delta = 0.01$.

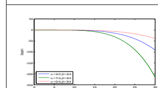

Figure 15: Graph of depth against time for values of $\alpha = {}^{3}/_{2}, \beta = {}^{3}/_{4},\ \alpha = {}^{7}/_{4}, \beta = {}^{3}/_{4}$ and $\alpha = {}^{5}/_{4}, \beta = {}^{3}/_{4}$. The parameters used are $a = 0.2, b = 1, c = 0.1, k = 6, m = 1, n = 2$ and $\delta = 0.01$.

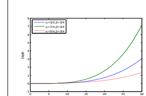

Figure 16: Graph of depth against time for values of $\alpha = {}^{3}/_{2}, \beta = {}^{3}/_{4},\ \alpha = {}^{7}/_{4}, \beta = {}^{3}/_{4}$ and $\alpha = {}^{5}/_{4}, \beta = {}^{3}/_{4}$. The parameters used are $a = -0.2, b = 1, c = 0.1, k = 6, m = 1, n = 2$ and $\delta = 0.01$.

oscillations gradually decay in amplitude towards zero. But a better result was obtained when we considered a fractional order model. It was observed from the simulations of the fractional order solution that for under-damped constant $a < 0$, the increase in depth with respect to time is clear, as shown in Figures 12, 14 and 15, and for damped constant $a > 0$, the decrease in depth with respect to time is also clear, as shown in Figures 11, 13 and 15. Therefore, the fractional order model has verified the significant effect of a climate change in a Pacific Ocean by showing clearly the increase or decrease in a depth of thermocline. We therefore recommend that this work will be of good use for flood prediction and mitigation policies for climate change.

References

[1] Z. Mohammad,Nonlinear Differential Equation Using a Multi-Step Laplace Adomian Decomposition.Annals of University of Craiova, Mathematics and Computer Sciences Vol. 39, No.2, 200-210, 2012.

[2] J. F. Gomeze-Aguilar, J. J. Rosale-Garcia, J. J. Bernal-Alvarado, T. Cordova-Fraga and R. Guzman-Cabrera, Fractional Mechanical Oscillators. Revista Mexicana de Fisica,Vol.58, 348 352, 2012.

[3] J. F.Gomez and D. Balealu, Solutions of the Telegraph Equations Using a Fractional Calculus Approach. The Publishing House of the Romanian Academy, 15, No.1, 27-34, 2014.

[4] A. D.Sergio, M. B. Jose and A. V. Carllos, Some Comments on Fractional Modeling and Numerical Simulations of Oscillations of Oscillatory Systems. 22nd International Congress of Mechanical Engineering (COBEM 2013), 9350-9359.
[5] R, Magin, Fractional Calculus in Bioengineering. Begell House Redding, 2006.
[6] J.S. Gajjar, Asymptotic Expansions and Perturbation Methods. Lecture note. University of Manchester, 2010. Available at http://www.maths.manchester.ac.uk gajjar/
[7] J. Fei-Fei, An Equatorial Ocean Recharge Paradigm for ENSO. Part I: Conceptual Model. Journal of the Atmospheric sciences,Vol.54, 811-829, 1997.
[8] W.B .White and Z. Liu, Non-linear Alignment of El Nio to the 11-Yr Solar Cycle. Geophys, 2008.Res.Lett. 35, L19607.doi:10.1029/2008GL034831.
[9] J. K. Rajapaksha, M. Satsuki, S. Lal, and G. Jagath, Multispectral Satellite Data on Ocean Surface to Predict its Temperature Vertical Profile; a Simple Model. Asian Journal of Geoinformatics, Vol.14, No.4, 23-29, 2014.
[10] S. Eric, D. Henk and G. Michael, Bifurcation Analysis of Ocean, Atmosphere and Climate Model, Handbook of Numerical Analysis, Research Gate, Vol.14, 2010.
[11] M. Scheffer, J.A. Carpenter, C. Folke, and B.Walker, Catastrophic Shifts in Ecosystem, Nature, Vol.413, 591-596, 2001.
[12] N. Stern, The Economics of Climate Change. The Stern Review. University Press, Cambridge, 2008.
[13] J.E. Hansen, Global Warming Twenty Years Later: Tipping Point Near. Available at: http://www.columbia.edu/jeh1/2008 twenty years later-20080623.pgf
[14] Americans Climate Choices: Panel on Advancing the Science of Climate Change, National Research Council. Available at: nas-sites.org¿acc ¿ panel-report.
[15] I. Arto, I. Capellan-perez, T. Filatova, M.Gonzalez-Eguinob, K. Hasselman, D.Kovalevsky, A. Markandya, S.Moghayer and M. Tarika, Review of Existing Literature on Methodologies to Model Nonlinearity Events in the Presence of Environment Tipping Points. Climate Mitigation Systems for a Low Carbon Economy, 2013.
[16] Thermocline (Global warming); see htt://what-when-how.com/global-warming/thermocline-global-warming/.
[17] S. Craig, Impacts of climate change on the physical oceanography of the Great Barrier Reef. Climate Change and the Great Barrier Reef: A Vulnerability Assessment, 51-74, 2007.
[18] K, Wyrtki, Water Displacements in the Pacific and the Genesis of El Nino Cycles. Journal of Geophysical Research,Vol. 90, 7129, 1985.
[19] A. Bershadskii, Nonlinear Problems of Complex Natural Systems: Sun and Climate Dynamics, 2013, Phil Trans R Soc A371: 20120168. http://dx.doi.org/10.1098/rsta.2012.0168
[20] M. O. Oyesanya and S. C. Eze, Perturbation Technique in Oceanic Climate Model with Damped Oscillations. Journal of the Nigerian Association of Mathematical Physics,Vol.43, 125-134, 2017.

S.C. Eze
Department of Mathematics, University of Nigeria, Nsukka, Nigeria
E-mail address: sundaychristianeze@gmail.com

M. O. Oyesanya
Department of Mathematics, University of Nigeria, Nsukka, Nigeria
E-mail address: moses.oyesanya@unn.edu.ng